

C.1.c.1.8-Copper Aluminum Layered Double Hydroxide Modified by.pdf

By Risfidian Mohadi

Original Article

Copper Aluminum Layered Double Hydroxide Modified by Biochar and its Application as an Adsorbent for Procion Red

Neza Rahayu Palapa ^a, Novie Juleanti ^c, Normah ^c, Risfidian Mohadi ^b, Tarmizi Taher ^d, Addy Rachmat ^b, Aldes Lesbani ^{a,c}

^a Graduate School of Mathematics and Natural Sciences, Sriwijaya University, Palembang, Indonesia

^b Department of Chemistry, Sriwijaya University, Indralaya, Indonesia

^c Research Center of Inorganic Materials and Coordination Complexes, Sriwijaya University, Indralaya, Indonesia

^d Institute of Regional Innovation, Hirosaki University, Hirosaki, Japan

ABSTRACT

The preparation of a copper aluminum/biochar composite and its application for the adsorption of procion red dye was studied. The composite materials were prepared by a co-precipitation method and characterised by X-ray diffraction, Fourier-transform infrared spectroscopy, Brunauer-Emmett-Teller surface area analysis, scanning electron microscopy, and thermogravimetry. The results of the adsorption study show that adsorption on the copper aluminum/biochar composite follows pseudo-second-order kinetics, and the adsorption isotherm of procion red conforms to the Langmuir isotherm model. The Langmuir fitting result for the maximum adsorption quantity of procion red on copper aluminum/biochar composite is 175.439 mg/g, which is higher than copper aluminum layered double hydroxide. The thermodynamic analysis suggests that procion red adsorption is spontaneous (standard free energy < 0) and endothermic and involves a random solid–liquid phase interface. The composite materials exhibited good recycling performance.

Keywords: layered double hydroxide, biochar, composite material, procion red, adsorption

INTRODUCTION

The textile and dyeing industry uses many kinds of synthetic dyes and disposes of large amounts of high-concentration coloured wastewater [1]. These wastes must be treated before they are discharged into raw water [2]. The stability of the chemical structure of dyes causes natural degradation and makes purification harder [3]. Although the concentration of dye is low, the colour may be infused in water [4]. The colour and concentration influence the natural life of aquatic ecosystems, thus damaging the ecological balance in water [5]. Most dyes can be hazardous for human beings, animals, and plants, with carcinogenic, teratogenic, and mutagenic effects [6]. Currently, the treatment of wastewater has become an emergency problem that needs to be solved. Various technologies and methods have been examined,

including advanced oxidation [7], membrane separation [8], ion exchange [9], and flocculation [5]. However, these methods have limitations such as low efficiency and high cost. The adsorption method has been shown to be effective for the treatment of dye pollution, because it is easy to operate, economical, and efficient. One of the most important aspects of the adsorption process is the selection of the adsorbent [10].

Several adsorbents have been reported to remove dyes from wastewater, such as bentonite [11], kaolin [12], chitosan [13], and layered double hydroxides (LDH) [14]. LDH is an inorganic layer material consisting of divalent (M^{2+}) and trivalent (M^{3+}) metal ions. A small anion, such as sulfate, nitrate, carbonate, or chloride, depending on the synthesis conditions used, is present between the cationic layers. The general formula of LDH is $[M^{2+}_{1-x}M^{3+}_x(OH)_2]^{x+}(A^{n-})$

Corresponding author: Aldes Lesbani, E-mail: aldeslesbani@pps.unsri.ac.id

Received: May 1, 2020, Accepted: August 12, 2020, Published online: December 10, 2020



Open Access This is an open-access article distributed under the terms of the Creative Commons Attribution (CC BY) 4.0 License. <http://creativecommons.org/licenses/by/4.0/>

Table 1 Composites of biochar and CuAl in CuAl/BC composites.

Samples	Biochar (g)	Cu:Al metal salts (g) (0.750:0.250) M
CuAl/BC composite 1:1	1	10.5:4.68
CuAl/BC composite 1:2	2	10.5:4.68

x/n] mH_2O where A^{n-} is the interlayer anion [15]. LDH has a net positive charge, and this charge is balanced by the interlayer anion. The use of LDH as an adsorbent for dyes has been studied by many researchers. MgFe-CO₃ LDH has been applied as a potential adsorbent for dyes such as Congo Red, with a maximum adsorption capacity of 104 mg/g [16]. Ca-Al LDH was examined as a high-efficiency adsorbent of Sunset Yellow [17]. Mg/Fe calcined LDH effectively removed Acid Brown 14, with a maximum adsorption capacity from pristine of 41.7 mg/g [18]. CuAl-NO₃ LDHs have been examined as adsorbents for cationic dyes, obtaining a maximum adsorption capacity of 59.52 mg/g [14].

Several methods have been studied to enhance the adsorption activity for dyes, such as LDH modifications. Lesbani and others [19] employed nickel-iron LDH intercalated with polyoxometalates to remove cationic dyes. The adsorption capacity of the modified LDH was higher than that of the pristine LDH. Composite formation by incorporating carbon-based compounds into LDH has also been used to enhance the adsorption capacity of LDH [20]. Biochar (BC) is a carbon-based compound obtained from the pyrolysis of biomass at a high temperature [21], and a composite BC material was used to remove dye pollutants from wastewater. Wan and co-workers [22] used MgFe-BC composites to remove phosphate, with removal percentages up to 95%. An Ni-Fe-BC pine composite has been employed as an arsenic removal agent, obtaining a maximum adsorption capacity of 4.38 g/kg [23]. Meili *et al.* [24] reported a composite of BC-bone with Mg/Al LDH, and the adsorption capacity obtained at a high temperature was 406 mg/g. Previous studies have shown that the coupling of BC with LDH is a favourable approach to producing high-performance, sustainable, and eco-economical adsorbent materials. Thus, the composites of LDH with BC produced from rice production wastes (rice husk) can act as versatile adsorbents for treatment of organic-contaminated wastewater, with inherent and exceptional ion exchangeability, high specific surface area, and low toxicity. Moreover, the use of waste from rice production can reduce the amount of biomass wasted. In this study, CuAl/BC composite materials were used to remove procion red (PR) dye. The effects of various conditions, including pH, time, initial

concentration, adsorption temperature, and regeneration of adsorbent effectivity were investigated, and the kinetics, isotherms, and thermodynamics of adsorption, desorption, and regeneration adsorption of PR on composite materials are discussed.

MATERIALS AND METHODS

Preparation of rice husk biochar

The starting material, rice husk, was obtained from local production in Central Java, Jogjakarta, Indonesia. The raw biomass was sun-dried before preparation for pyrolysis treatment. The pyrolysis was conducted in a furnace under constant N₂ flow for two hours at 500°C, with a reactor heating rate of 10°C/min. After the reactor had cooled to room temperature, BC from the rice husk was removed from the furnace and characterised.

Preparation of the CuAl/BC composite

CuAl LDH was synthesised according to a previously reported method [14]. The composite material was prepared by mixing 50 mL of 0.750 M copper nitrate (10.5 g; Merck Darmstadt, Germany) with 50 mL of 0.250 M aluminum nitrate (4.68 g; Merck, Darmstadt, Germany). The mixture was stirred constantly for 1 h until complete dissolution of the starting materials. The amount of BC shown in Table 1 was added to 50 mL deionised water and mixed for 1 h before being transferred into a reaction flask. A solution of 1 M sodium hydroxide (Merck, Darmstadt, Germany) was added dropwise until the pH was 10. The mixture was kept at 80°C for three days, after which the composite was separated by centrifugation for 15 min (500 rpm), and the solid was dried in air at room temperature for a day. The characterisation of the prepared materials was performed as follows: powder X-ray diffraction (XRD) using a Rigaku Miniflex-600 diffractometer, scanning at 1°/min; Fourier-transform infra-red spectrometry (FTIR) with a Shimadzu Prestige-21 spectrometer on a KBr disc, scanning wavenumbers 400–4,000 1/cm; morphology analysis using a Quanta-650 scanning electron microscope (SEM) with an Oxford Instruments detector; and thermal analysis using a Shimadzu DTG-60H (Shimadzu

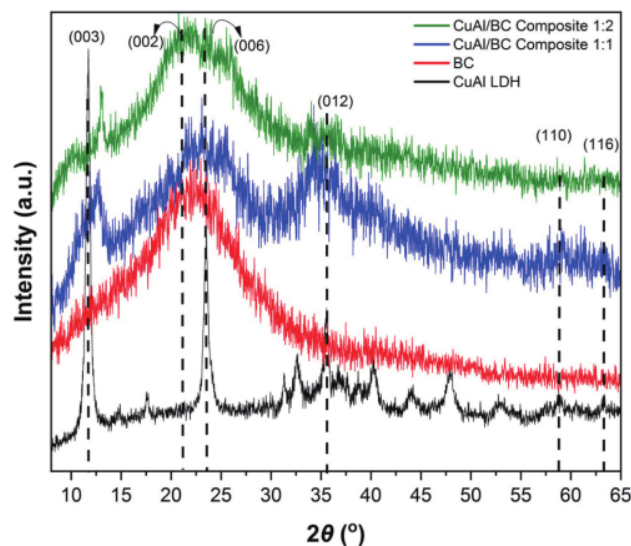


Fig. 1 PXRD of CuAl LDH, BC and composite materials.

Scientific Instruments, Kyoto, Japan), which measures the change in sample weight under nitrogen gas and controlled temperature ranging from 20 to 1,000°C.

Adsorption and regeneration studies

The adsorption process was carried out in batches. A 0.050 g portion of the prepared material was added to 50 mL of PR solution. The adsorption study was conducted by varying the adsorption time, initial concentration, and adsorption temperature. The desorption study was performed using several reagents, including NaOH, HCl, water, and ethanol. The adsorbed material (0.250 g) and reagent (25 mL) were mixed and the mixture shaken for 90 min. The filtrate was separated by centrifugation at 100 rpm and the adsorbate was measured. The regeneration study was carried out by adding 0.250 g of adsorbent to 100 mL PR solution (100 mg/L) and shaking the mixture for 2 h. The adsorbent was separated from the adsorbate, and the remaining adsorbate was analysed using the UV-Vis spectrophotometer Bio-Base BK-UV1800 (Biobase Biodustry Co., Ltd., Shandong, China) at a wavelength of 536 nm. The dried adsorbent was reused for four cycles with a similar procedure.

RESULTS AND DISCUSSION

The XRD patterns of the CuAl LDH, BC, and composite materials are shown in Fig. 1. The XRD pattern of the CuAl

LDH shows the characteristic reflections due to the 003, 006, 012, 110, and 116 planes corresponding to the layered structure of CuAl LDH, confirmed by JCPDS No. 73–6300. The basal spacing of CuAl LDH at $2\theta = 12.016^\circ$, the (003) reflection, is 7.543 Å. The broad (002) reflection peak is characteristic of carbon compounds [25]. The characteristic peaks of pristine LDH and BC appeared in the XRD pattern of the CuAl/BC composite, although in the composite materials the crystallinity of LDH was reduced, which may result from breakage of the LDH structure leading to a reduction and shift of the LDH (003) reflections. The strong reflections of CuAl LDH observed at a BC content of 1 g were observed at 2 g with a slight reduction in peak intensities. This indicates that the crystalline structure of the composites slightly deviated with the incorporation of increased BC [26].

The FTIR spectra of the CuAl LDH, BC, and composite materials are presented in Fig. 2. The intense, broad bands at 3,400 $1/\text{cm}$ are due to O–H stretching vibrations, whereas the 1,635 $1/\text{cm}$ band corresponds to O–H bending of water molecules. The sharp peak at 1,381 $1/\text{cm}$, assigned to the interlayer nitrate anion, was observed with a reduced intensity in the CuAl/BC composite. An absorption band at 1,095 $1/\text{cm}$ in the composite is assigned to a C–O stretching vibration [22]. The presence of the characteristics bands of both starting materials confirms the successful preparation of the CuAl/BC composite.

The results of the N_2 adsorption–desorption isotherms of

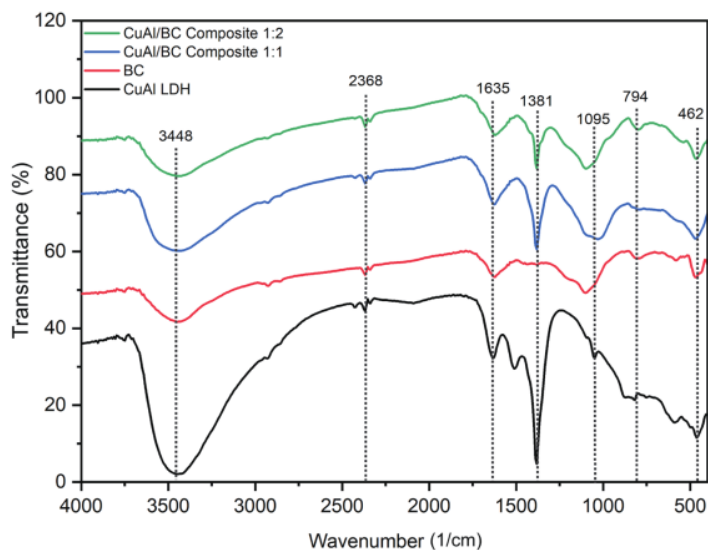


Fig. 2 FTIR spectrum of CuAl LDH, BC and composite materials.

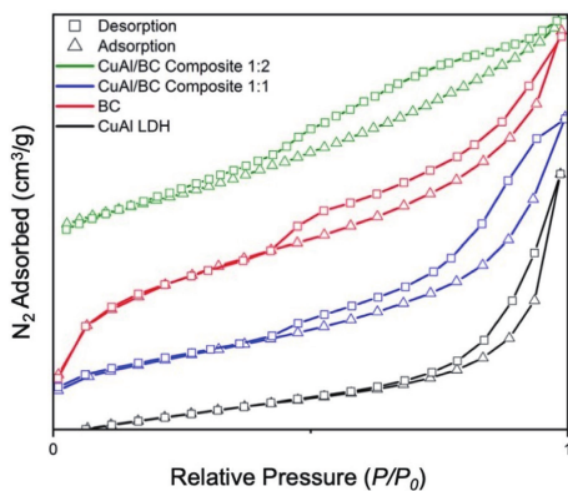


Fig. 3 N₂ adsorption-desorption curve of CuAl LDH, BC and composite materials.

CuAl LDH, BC, and the composite materials are shown in Fig. 3. The isotherms of the prepared materials are of Type IV in the IUPAC classification, which indicates capillary condensation within the mesopores. The hysteresis loops of these materials are of H3 type at high relative pressures P/P_0 , which implies the presence of slit-shaped pores created by an aggregate particle non-rigid mode. All pore sizes

are typical of mesoporous materials with pore diameters in the range 2–50 nm [27]. Table 2 also shows that an increase in the surface area of the CuAl/BC composite is associated with a decrease in pore size. The CuAl/BC 1:2 composite obtained in this experiment shows a higher surface area than the others according to the Brunauer-Emmett-Teller (BET) measurements. Based on Table 2, CuAl/BC 1:2 composite

Table 2 Textural properties of CuAl LDH, BC and composite materials.

Materials	BET Surface (m ² /g)	Pore Size (nm)	Pore Volume (cm ³ /g)
BC	72.251	3.334	0.060
CuAl	46.279	10.39	0.116
CuAl/BC composite 1:1	200.90	7.032	0.350
CuAl/BC composite 1:2	228.87	6.351	0.404

has a lower pore size and larger surface area compared with pristine LDH, where the values were 6.351 nm and 228.87 m²/g, respectively. The CuAl/BC composite material had a different ratio, with increased surface area and decreased pore size. The decrease in pore size occurs due to the composite sites of BC particles within the LDH layers. This can be attributed to the intercalation of BC within the LDH layers, leading to the formation of larger pores, which can act as active binding sites; higher removal of PR molecules can be expected. Similar results have been found [28] showing that BC is not a porous material and has a low BET porous size and volume size. According to Harizi *et al.* [29], the alteration of pore size after the modification of LDH can be understood by assuming the removal of water in the interlayer. The intercalated nitrate anions of the initially synthesised LDH led to the formation of channels and pores.

The SEM/energy-dispersive X-ray spectroscopy (SEM/EDX) images of CuAl LDH, BC, and the composite materials are shown in Fig. 4. CuAl LDH displays aggregate structures formed of particles, which are typical of CuAl LDH prepared by the co-precipitation method [30]. The EDX analysis provides information about the existence of other ions in the CuAl LDH interlayer space, such as CO₃²⁻. Moreover, as seen from the SEM/EDX images of the composite materials (Figs. 4c and 4d), the carbon and oxygen contents increased for the CuAl/BC composite, which indicates the appearance of BC and a decrease in the contribution from the CuAl LDH structure. Similar composite materials were reported by Wang *et al.* [31] who reported that the surface morphology of biochar-modified LDH has no particular structure and predominantly reveals the presence of the LDH phase.

Thermogravimetry with differential thermal analysis (TG-DTA) of CuAl LDH, BC, and the composite materials was carried out to investigate the thermal stabilities of the materials. As shown in Fig. 5a, the TG-DTA of CuAl LDH exhibits a two-stage weight loss. The first stage occurred in the range 50–240°C due to the loss of water molecules from the surface and interlayer space, whereas the second

can be attributed to structural compromise of the layered structure of LDH. Similar findings were reported by Parida and Mohapatra [32], who observed an endothermic peak related to the weight loss of water molecules at 150–250°C, and a second region where the layered structure of LDH broke up. Figure 5b shows two steps of weight loss. The first step is the loss of water between 25 and 100°C, mainly due to moisture evaporation. The second is a significant weight loss at 100–520°C, and no weight loss was detected thereafter. Weight loss above 100°C was caused by devolatilisation and char combustion. This process, according to Mohapatra *et al.* [33] is manifested in major loss of weight and is attributed to the fact that carbon is oxidised, and this oxidation process is completed at 700°C. The composite materials undergo similar weight losses. Figures 5c and 5d show the first step, which is the weight loss of water molecules in the composite materials. The slight decreases in weight loss from carbon and the LDH interlayer disappeared.

Adsorption study

Contact time is an important parameter in the adsorption process. Figure 6 shows that the dye uptake increased slightly with time and thereafter reached equilibrium. The adsorption contact time for PR solution using all adsorbents was 90 minutes, with equilibrium adsorption capacity of 17.089 mg/g for CuAl LDH, 20.886 mg/g for BC, 24.051 mg/g for the CuAl/BC 1:1 composite, and 25.570 mg/g for the CuAl/BC 1:2 composite. In terms of the ideas outlined by Berber-Villamar *et al.* [34], the LDH adsorption ability is due to the availability of the binding site for adsorption and the high driving force that occurs in the initial contact time to move the dye molecule in the solution to the adsorbent surface.

The kinetics of PR adsorption onto CuAl LDH, BC, and the composite materials was examined using the two most studied kinetic models: the pseudo-first-order (PFO) and pseudo-second-order (PSO) models. These models can be expressed as follows:

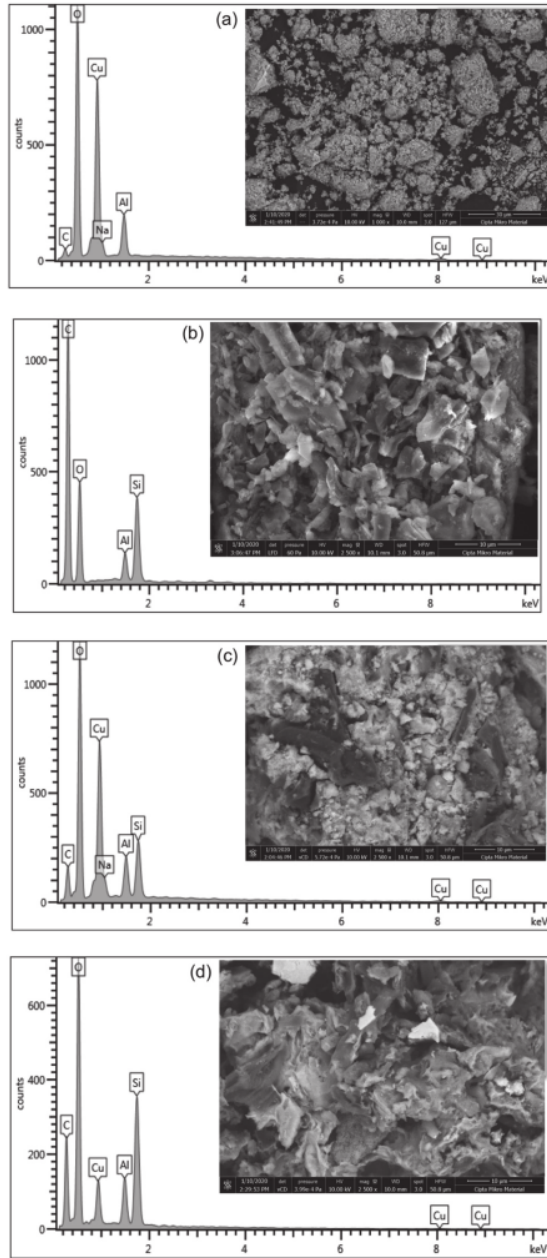


Fig. 4 SEM-EDX images of (a) CuAl LDH, (b) BC, (c) CuAl/BC composite 1:1 and (d) CuAl/BC composite 1:2.

$$\log (q_e - q_t) = \log q_e - \left(\frac{k_1}{2,303} \right) t \quad (1)$$

$$\frac{t}{q_t} = \frac{1}{k_2 q_e^2} + \frac{1}{q_e} t \quad (2)$$

q_e = adsorption capacity at equilibrium (mg/g)

q_t = adsorption capacity at t (mg/g)

t = adsorption time (min)

k_1 = adsorption kinetic rate at PFO (1/min)

k_2 = adsorption kinetic rate at PSO (g/mg.min)

The fitted model values and the experimental data are presented in **Fig. 6**, and the calculated kinetic parameters of PR adsorption are presented in **Table 3**. **Table 3** shows the results of calculations using equations (1) (PFO) and (2) (PSO) based on the experimental data. All materials follow the PSO kinetic model based on a correlation coefficient (R^2) > 0.991. The adsorption capacity of the adsorbent based on the PSO model is very close to the experimental value, as depicted in **Fig. 6**. This finding suggests that the adsorption process can be assumed to occur by chemical interactions, or chemisorption. Similar results were reported by Harizi *et al.* [29], where finding that the adsorption kinetics best fitted PSO rather than PFO indicated the chemisorption mechanism.

The adsorption equilibrium was investigated at different initial concentrations. The adsorption isotherms of PR, using CuAl LDH, BC, and the composite materials, are shown in **Table 4**. The isotherm parameters calculated according to the Langmuir and Freundlich isotherm models are formulated as follows:

$$\frac{1}{q_e} = \frac{1}{q_{max}} + \frac{1}{q_{max} b} \cdot \frac{1}{C_e} \quad (3)$$

$$\ln q_e = \ln K_f + \left(\frac{1}{n} \right) \ln C_e \quad (4)$$

q_{max} = the maximum adsorption capacity conducted in the monolayer (mg/g)

b = the Langmuir adsorption equilibrium constant (1/mg)

C_e = the equilibrium concentration (mg/L)

K_f = Freundlich constant

Furthermore, the Langmuir parameters can be used to predict whether the adsorption is favourable. The parameters of the two models were calculated by plotting q_e vs. C_e in several

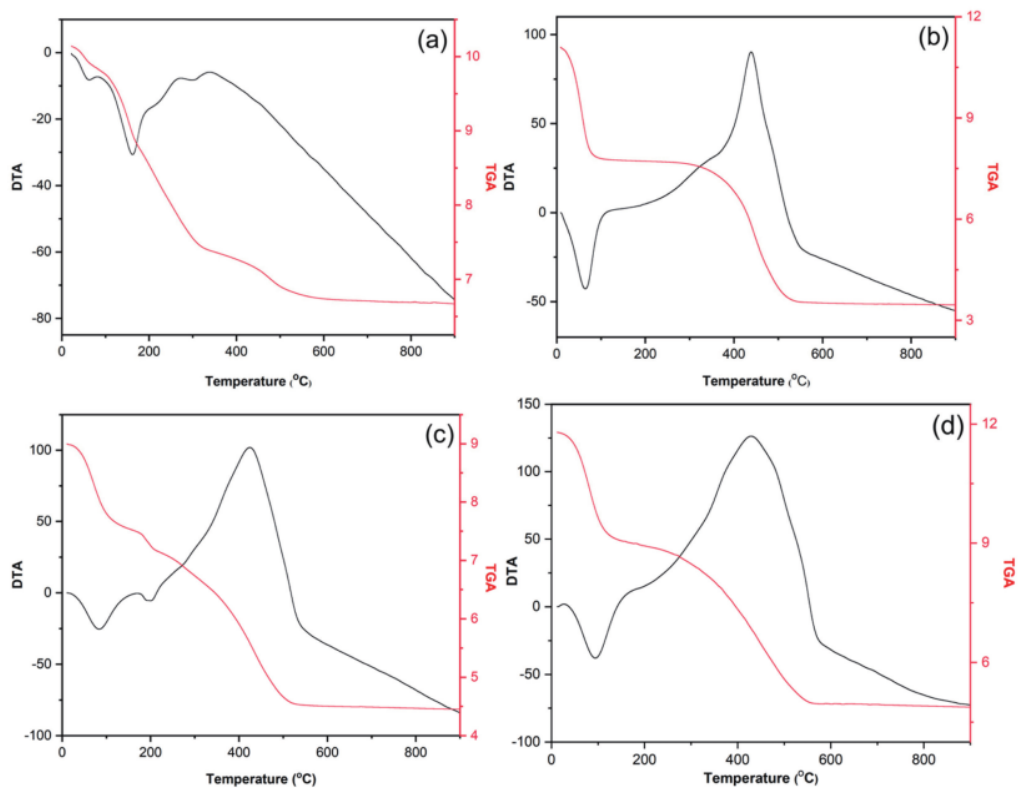


Fig. 5 TG-DTA profile of (a) CuAl LDH, (b) BC, (c) CuAl/BC composite 1:1 and (d) CuAl/BC composite 1:2.

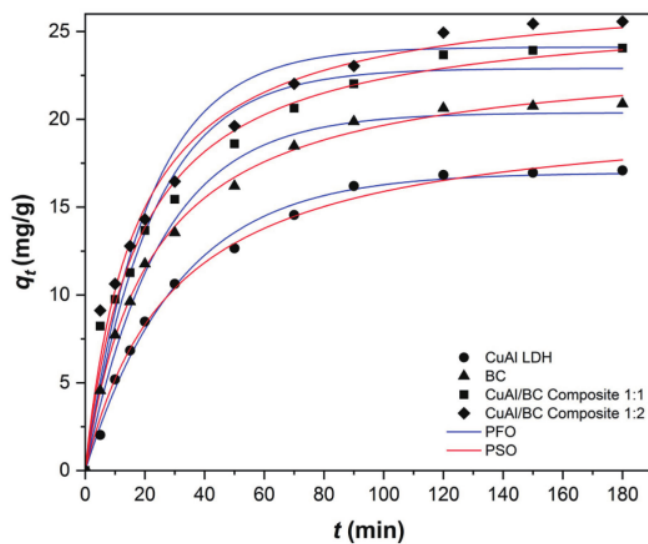


Fig. 6 The plot of the fitted kinetics model against the experimental data.

Table 3 Adsorption kinetics parameters of PR onto adsorbents.

Adsorbent	$Qe_{\text{experiment}}$ (mg/g)	PFO			PSO		
		Qe_{Calc} (mg/g)	R^2	k_1 (1/min)	Qe_{Calc} (mg/g)	R^2	k_2 (g/(mg · min))
CuAl LDH	17.089	18.022	0.989	0.033	20.704	0.991	0.001
BC	20.886	20.244	0.992	0.034	21.332	0.996	0.013
CuAl/BC composite 1:1	24.051	22.808	0.976	0.032	25.907	0.991	0.002
CuAl/BC composite 1:2	25.570	23.637	0.962	0.031	24.272	0.992	0.002

Table 4 Langmuir and Freundlich isotherm parameters for the adsorption of PR onto adsorbents.

LDH	Adsorption Isotherm	Adsorption Constant	T (°C)			
			30	40	50	60
CuAl LDH	Langmuir	q_{max}	64.935	66.225	67.114	68.493
		b	0.169	0.120	0.088	0.100
		R^2	0.998	0.998	0.997	0.999
	Freundlich	n	4.158	3.503	3.055	3.049
		K_f	23.988	19.530	15.907	16.869
		R^2	0.998	0.990	0.992	0.971
BC	Langmuir	q_{max}	65.789	67.114	71.429	71.942
		b	0.223	0.091	0.072	0.054
		R^2	0.984	0.987	0.998	0.992
	Freundlich	n	4.394	3.085	2.883	2.290
		K_f	26.959	16.185	14.716	10.151
		R^2	0.926	0.974	0.959	0.993
CuAl/BC composite 1:1	Langmuir	q_{max}	70.922	74.074	90.909	147.70
		b	0.116	0.058	0.012	0.012
		R^2	0.999	0.982	0.999	0.968
	Freundlich	n	3.221	2.132	1.001	1.367
		K_f	19.222	8.722	1.009	3.183
		R^2	0.994	0.984	0.999	0.998
CuAl/BC composite 1:2	Langmuir	q_{max}	72.464	84.034	91.743	175.43
		b	0.058	0.027	0.030	0.008
		R^2	0.985	0.996	0.988	0.986
	Freundlich	n	2.446	1.815	1.823	1.203
		K_f	11.329	5.705	6.693	2.052
		R^2	0.979	0.999	0.991	0.998

adsorbents with the same concentration. **Table 4** presents the calculated correlation coefficients, which indicate that the Langmuir model is better fitted than the Freundlich model for composite materials. The maximum adsorption capacity of the CuAl/BC 1:2 composite was 175.43 mg/g, which is higher than those of CuAl LDH (68.493 mg/g), BC (71.942 mg/g), and the CuAl/BC 1:1 composite (147.70 mg/g). The PR adsorption capacities of the CuAl/BC composites were also

higher than those of pristine BC. This further confirms that the significant increase in the dye removal performance of **BC** resulting from the modification of CuAl LDH with BC is associated with the synergetic effect of BC and CuAl in the composite, and hence that the surface area of the CuAl/BC 1:2 composite was larger.

The effects of temperature on the adsorption of PR by CuAl, BC, and the composite materials are shown in **Fig.**

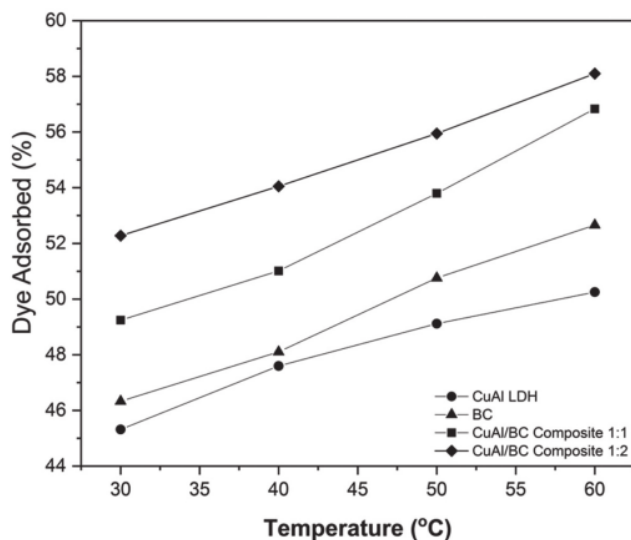


Fig. 7 Effect of adsorption temperature of PR onto CuAl, BC and composite materials.

7. The amount of PR adsorbed increased with the temperature; the amount adsorbed from the initial concentration of 90.823 mg/L by the CuAl/BC 1:2 composite was 57.951%, and by the 1:1 composite, 55.808%. The thermodynamic parameters of the adsorption process, such as the changes in standard Gibbs free energy (ΔG), enthalpy (ΔH), and entropy (ΔS), were obtained from experiments at various temperatures using the following equations:

$$\Delta G = -RT \ln K_D \quad (5)$$

$$\ln K_D = \frac{S}{R} - \frac{H}{RT} \quad (6)$$

K_D = the distribution coefficient

R = the molar gas constant

T = the absolute temperature (K)

ΔH = Enthalpy (kJ/mol)

ΔS = Entropy (kJ/mol)

ΔG = Gibbs free energy (kJ/mol)

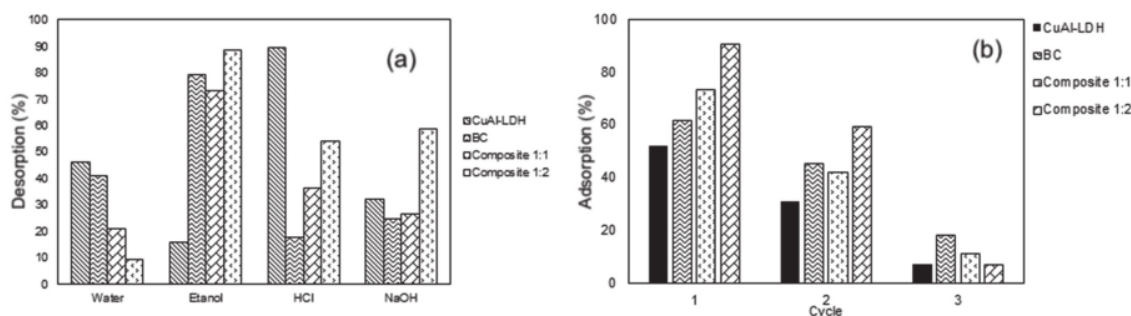
ΔS and ΔH were calculated from the slope and intercept of the van't Hoff plots of $\ln K_D$ vs. $1/T$. Table 5 shows the calculated values of the thermodynamic parameters. Lower values of energy and enthalpy, in the range 5–40 kJ/mol, indicate physical sorption, and values higher than 40 indicate chemical sorption. According to Table 5, the adsorption of PR onto

all adsorbents requires lower energy, suggesting physical sorption. The negative value of ΔG at various temperatures implies that the adsorption process is spontaneous. Endothermic adsorption was also confirmed by the ΔH values. ΔH and ΔS with the liquid phase were influenced by various conditions such as temperature, concentration, and interaction between liquid and solid interfaces during the adsorption process. In addition, the effect of temperature on the adsorption phenomena was also found to depend on the viscosity of the solvent, which with PR will lead to the mobility of the solute at higher temperatures. Thus, the adsorption might be favourable and have a high capacity at high temperatures. In addition, based on previous results, it is confirmed that the adsorption process leads to the Langmuir isotherm, which indicates adsorption of a monolayer on the surface, although the high adsorption capacity might suggest the formation of multiple layers. As previously reported [35], for dye systems, the Langmuir assumptions of infinite dilution and monolayer saturation apply to gas systems with uniform sites and no interaction between monolayer adsorbed molecules on a homogeneous surface. Furthermore, Table 5 also shows that the CuAl/BC 1:2 composite had the highest adsorption capacity value, indicating that the interaction of the adsorbate and the adsorbent led to more effective adsorption of PR.

In order to increase the effectiveness of the potential adsorbent, a regeneration study is necessary. The adsorbent

Table 5 Values of thermodynamic parameters for PR adsorption by CuAl, BC and composite materials.

Adsorbent	C_{initial} (mg/L)	T (°C)	ΔH (kJ/mol)	ΔS (kJ/mol)	ΔG (kJ/mol)
CuAl LDH	90.823 mg/L	30	6.078	0.020	-0.016
		40			-0.217
		50			-0.419
		60			-0.620
BC	90.823 mg/L	30	8.065	0.027	-0.081
		40			-0.350
		50			-0.619
		60			-0.887
CuAl/BC composite 1:1	90.823 mg/L	30	9.701	0.033	-0.376
		40			-0.708
		50			-1.041
		60			-1.373
CuAl/BC composite 1:2	90.823 mg/L	30	15.419	0.053	-0.587
		40			-1.116
		50			-1.644
		60			-2.172

**Fig. 8** Desorption (a) and regeneration (b) of PR adsorption by CuAl, BC and composite materials.

reusability evaluation was carried out with several reagents for the desorption of PR from CuAl LDH, BC, and the composite materials. The results of the regeneration experiments after three cycles of adsorption–desorption are shown in Fig. 8. The efficiency of dye removal decreased from 92.643% to 8.125% for the 1:2 CuAl/BC composite, from 72.783% to 15.062% for the 1:1 CuAl/BC composite, from 62.188% to 20.553% for BC, and from 50.546% to 6.103% for CuAl LDH. CuAl LDH had the lowest efficiency after the third regeneration because CuAl LDH dissolves in the acidic reagent and, hence, is not feasible for reuse. According to Nishimura and co-workers [36], LDHs treated in regeneration processes might suffer damage to their structure due to

exfoliation. However, the composite materials prepared in this work can be reused, although their adsorption capacity is slightly reduced.

CONCLUSIONS

In this study, CuAl/BC composites with gram ratios of 1:1 and 1:2 were prepared and applied to adsorb PR. The surface area of CuAl/BC increased with the proportion of BC, to 200.90 m²/g for CuAl/BC (1:1) and 228.87 m²/g for CuAl/BC (1:2). The FTIR spectrum and XRD pattern also confirmed that the presence of BC conferred unique characteristics on the composites. The adsorption of PR on the composite

material and pristine material increased rapidly and reached equilibrium after 90 min with dye uptake of 24.051 mg/g for CuAl/BC (1:1) and 25.570 mg/g for CuAl/BC (1:2). The adsorption kinetics followed the PSO model with a correlation coefficient close to unity. The adsorption isotherms could be effectively fitted using the Langmuir model. The Langmuir fitting indicated that the q_{max} values for PR adsorption on the 1:1 and 1:2 CuAl/BC composites were 147.70 and 175.43 mg/g, respectively. The thermodynamic analysis showed that PR adsorption on all adsorbents was spontaneous ($\Delta G < 0$) and endothermic, and involved randomness of the solid-liquid phase interface. Furthermore, the composite materials exhibited good recycling performance.

ACKNOWLEDGMENT

This research was supported by Sriwijaya University, which provided funding through "Hibah Profesi dana PNBPN" in the fiscal year 2020. Author thank to Research Centre of Inorganic Materials and Complexes FMIPA Sriwijaya University for supporting instrumentation and analysis.

REFERENCES

- [1] Daud M, Hai A, Banat F, Wazir MB, Habib M, Bharath G, Al-Harhi MA: A review on the recent advances, challenges and future aspect of layered double hydroxides (LDH) – Containing hybrids as promising adsorbents for dyes removal. *Journal of Molecular Liquids*, **288**, 110989, 2019. doi:10.1016/j.molliq.2019.110989
- [2] Nidheesh PV, Zhou M, Oturan MA: An overview on the removal of synthetic dyes from water by electrochemical advanced oxidation processes. *Chemosphere*, **197**, 210–227, 2018. PMID:29366952 doi:10.1016/j.chemosphere.2017.12.195
- [3] Hu H, Wageh S, Al-Ghamdi AA, Yang S, Tian Z, Cheng B, Ho W: NiFe-LDH nanosheet/carbon fiber nanocomposite with enhanced anionic dye adsorption performance. *Applied Surface Science*, **511**, 145570, 2020. doi:10.1016/j.apsusc.2020.145570
- [4] Gao M, Wang Z, Yang C, Ning J, Zhou Z, Li G: Novel magnetic graphene oxide decorated with persimmon tannins for efficient adsorption of malachite green from aqueous solutions. *Colloids and Surfaces A: Physicochemical and Engineering Aspects*, **566**, 48–57, 2019. doi:10.1016/j.colsurfa.2019.01.016
- [5] Shankar YS, Ankur K, Bhushan P: Utilization of Water Treatment Plant (WTP) Sludge for Pretreatment of Dye Wastewater Using Coagulation/ Flocculation. Springer, Singapore, 2019. doi:10.1007/978-981-13-0215-2_8
- [6] Srivastava S, Sinha R, Roy D: Toxicological effects of malachite green. *Aquat. Toxicol.*, **66**(3), 319–329, 2004. PMID:15129773 doi:10.1016/j.aquatox.2003.09.008
- [7] Shukla SR, Pai RS, Shendarkar AD: Adsorption of Ni(II), Zn(II) and Fe(II) on modified coir fibres. *Separ. Purif. Tech.*, **47**(3), 141–147, 2006. doi:10.1016/j.seppur.2005.06.014
- [8] Xu Y, Li Z, Su K, Fan T, Cao L: Mussel-inspired modification of PPS membrane to separate and remove the dyes from the wastewater. *Chemical Engineering Journal*, **341**, 371–382, 2018. doi:10.1016/j.cej.2018.02.048
- [9] Fu F, Wang Q: Removal of heavy metal ions from wastewaters: A review. *J. Environ. Manage.*, **92**(3), 407–418, 2011. PMID:21138785 doi:10.1016/j.jenvman.2010.11.011
- [10] Chilukoti S, Thangavel T: Enhanced adsorption of Congo red on microwave synthesized layered Zn-Al double hydroxides and its adsorption behaviour using mixture of dyes from aqueous solution. *Inorg. Chem. Commun.*, **100**(February, 2018), 107–117, 2019. doi:10.1016/j.inoche.2018.12.027
- [11] Niu M, Li G, Cao L, Wang X, Wang W: Preparation of sulphate aluminate cement amended bentonite and its use in heavy metal adsorption. *Journal of Cleaner Production*, **256**, 120700, 2020. doi:10.1016/j.jclepro.2020.120700
- [12] Abidi N, Duplay J, Jada A, Errais E, Ghazi M, Semhi K, Trabelsi-Ayadi M: Removal of anionic dye from textile industries' effluents by using Tunisian clays as adsorbents. Zeta potential and streaming-induced potential measurements. *Comptes Rendus Chimie*, **22**(2–3), 113–125, 2019. doi:10.1016/j.crci.2018.10.006
- [13] Bekçi Z, Özveri C, Seki Y, Yurdakoç K: Sorption of malachite green on chitosan bead. *J. Hazard. Mater.*, **154**(1–3), 254–261, 2008. PMID:18022317 doi:10.1016/j.jhazmat.2007.10.021
- [14] Palapa NR, Mohadi R, Rachmat A, Lesbani A: Adsorption study of malachite green removal from aqueous solution using Cu/M3+ (M3+=Al, Cr) layered double hydroxide. *Mediterranean Journal of Chemistry*, **10**(1), 33–45, 2020. doi:10.13171/mjc10102001261236al

- [15] Mishra G, Dash B, Pandey S: Layered double hydroxides : A brief review from fundamentals to application as evolving biomaterials. *Appl. Clay Sci.*, **153**(October 2017), 172–186, 2018.
- [16] Ahmed IM, Gasser MS: Adsorption study of anionic reactive dye from aqueous solution to Mg–Fe–CO₃ layered double hydroxide (LDH). *Applied Surface Science*, **259**, 650–656, 2012. doi:10.1016/j.apsusc.2012.07.092
- [17] de Sá FP, Cunha BN, Nunes LM: Effect of pH on the adsorption of Sunset Yellow FCF food dye into a layered double hydroxide (CaAl-LDH-NO₃). *Chemical Engineering Journal*, **215–216**, 122–127, 2013. doi:10.1016/j.cej.2012.11.024
- [18] Guo Y, Zhu Z, Qiu Y, Zhao J: Enhanced adsorption of acid brown 14 dye on calcined Mg/Fe layered double hydroxide with memory effect. *Chemical Engineering Journal*, **219**, 69–77, 2013. doi:10.1016/j.cej.2012.12.084
- [19] Lesbani A, Taher T, Palapa NR, Mohadi R, Rachmat A, Mardiyanto : Preparation and utilization of Keggin-type polyoxometalate intercalated Ni–Fe layered double hydroxides for enhanced adsorptive removal of cationic dye. *SN Applied Sciences*, **2**(3), 470–473, 2020. doi:10.1007/s42452-020-2300-8
- [20] Chen J: Host-guest functional materials. *Modern Inorganic Synthetic Chemistry*, **2**, 405–428, 2011. doi:10.1016/B978-0-444-53599-3.10018-6
- [21] Silos-Llamas AK, Durán-Jiménez G, Hernández-Montoya V, Montes-Morán MA, Rangel-Vázquez NA: Understanding the adsorption of heavy metals on oxygen-rich biochars by using molecular simulation. *Journal of Molecular Liquids*, **298**, 112069, 2020. doi:10.1016/j.molliq.2019.112069
- [22] Wan S, Wang S, Li Y, Gao B: Functionalizing biochar with Mg–Al and Mg–Fe layered double hydroxides for removal of phosphate from aqueous solutions. *Journal of Industrial and Engineering Chemistry*, **47**, 246–253, 2017. doi:10.1016/j.jiec.2016.11.039
- [23] Wang S, Gao B, Li Y, Zimmerman AR, Cao X: Sorption of arsenic onto Ni/Fe layered double hydroxide (LDH)-biochar composites. *RSC Advances*, **6**(22), 17792–17799, 2016. doi:10.1039/C5RA17490B
- [24] Meili L, Lins PV, Zanta CLPS, Soletti JI, Ribeiro LMO, Dornelas CB, Silva TL, Vieira MGA: MgAl-LDH/Biochar composites for methylene blue removal by adsorption. *Appl. Clay Sci.*, **168**(May 2018), 11–20, 2019. doi:10.1016/j.clay.2018.10.012
- [25] Wang T, Li C, Wang C, Wang H: Biochar/MnAl-LDH composites for Cu (II) removal from aqueous solution. *Colloids and Surfaces A: Physicochemical and Engineering Aspects*, **538**, 443–450, 2018. doi:10.1016/j.colsurfa.2017.11.034
- [26] Zubair M, Jarrah N, Manzar MS, Al-Harhi M, Daud M, Mu'azu ND, Haladu SA: Adsorption of eriochrome black T from aqueous phase on MgAl-, CoAl- and NiFe- calcined layered double hydroxides: Kinetic, equilibrium and thermodynamic studies. *Journal of Molecular Liquids*, **230**, 344–352, 2017. doi:10.1016/j.molliq.2017.01.031
- [27] Monte Blanco SPD, Scheufele FB, Módenes AN, Espinoza-Quiñones FR, Marin P, Kroumov AD, Borba CE: Kinetic, equilibrium and thermodynamic phenomenological modeling of reactive dye adsorption onto polymeric adsorbent. *Chemical Engineering Journal*, **307**, 466–475, 2017. doi:10.1016/j.cej.2016.08.104
- [28] Azargohar R, Dalai AK: Biochar as a precursor of activated carbon. *Applied Biochemistry and Biotechnology*, **131**(1–3), 762–773, 2006. doi:10.1385/ABAB:131:1:762
- [29] Harizi I, Chebli D, Bouguettoucha A, Rohani S, Amrane A: A new Mg–Al–Cu–Fe-LDH composite to enhance the adsorption of acid red 66 dye: Characterization, kinetics and isotherm analysis. *Arabian Journal for Science and Engineering*, **44**(6), 5245–5261, 2019. doi:10.1007/s13369-018-3526-2
- [30] Bukhtiyarova MV: A review on effect of synthesis conditions on the formation of layered double hydroxides. *J. Solid State Chem.*, **269**(October 2018), 494–506, 2019. doi:10.1016/j.jssc.2018.10.018
- [31] Wang B, Qu J, Li X, He X, Zhang Q: Precursor preparation to promote the adsorption of Mg-Al layered double hydroxide. *Journal of the American Ceramic Society*, **2885**, 2882–2885, 2016. doi:10.1111/jace.14404
- [32] Parida KM, Mohapatra L: Carbonate intercalated Zn/Fe layered double hydroxide: A novel photocatalyst for the enhanced photo degradation of azo dyes. *Chemical Engineering Journal*, **179**, 131–139, 2012. doi:10.1016/j.cej.2011.10.070
- [33] Mohapatra S, Sakthivel R, Roy GS, Varma S, Singh SK, Mishra DK: Synthesis of β-SiC powder from bamboo leaf in a DC extended thermal plasma reactor. *Mater. Manuf. Process.*, **26**(11), 1362–1368, 2011. doi:10.1080/10426914.2011.557127

- [34] Berber-Villamar NK, Netzahuatl-Muñoz AR, Morales-Barrera L, Chávez-Camarillo GM, Flores-Ortiz CM, Cristiani-Urbina E: Corncob as an effective, eco-friendly, and economic biosorbent for removing the azo dye Direct Yellow 27 from aqueous solutions. *PLoS One*, **13**(4), e0196428, 2018. PMID:29698442 doi:10.1371/journal.pone.0196428
- [35] Ribeiro C, Scheufele FB, Espinoza-Quñones FR, Módenes AN, da Silva MGC, Vieira MGA, Borba CE: Characterization of *Oreochromis niloticus* fish scales and assessment of their potential on the adsorption of reactive blue 5G dye. *Colloids and Surfaces A: Physicochemical and Engineering Aspects*, **482**, 693–701, 2015. doi:10.1016/j.colsurfa.2015.05.057
- [36] Nishimura S, Takagaki A, Ebitani K: Monodisperse iron oxide nanoparticles embedded in Mg-Al hydro-talcite as a highly active, magnetically separable, and recyclable solid base catalyst. *Bulletin of the Chemical Society of Japan*, **83**(7), 846–851, 2010. doi:10.1246/bcsj.20100059

C.1.c.1.8-Copper Aluminum Layered Double Hydroxide Modified by.pdf

ORIGINALITY REPORT

4%

SIMILARITY INDEX

PRIMARY SOURCES

- 1 Mukarram Zubair, Mohammad Saood Manzar, Nuhu Dalhat Mu'azu, Ismail Anil, Nawaf I. Blaisi, Mamdouh A. Al-Harhi. "Functionalized MgAl-layered hydroxide intercalated date-palm biochar for Enhanced Uptake of Cationic dye: Kinetics, isotherm and thermodynamic studies", Applied Clay Science, 2020

172 words — 4%

[Crossref](#)

EXCLUDE QUOTES OFF

EXCLUDE MATCHES < 3%

EXCLUDE BIBLIOGRAPHY ON